Observation of a Charmoniumlike State Produced in Association with a J/ψ in e^+e^- Annihilation at $\sqrt{s} \approx 10.6$ GeV

K. Abe,[7] I. Adachi,[7] H. Aihara,[40] K. Arinstein,[1] Y. Asano,[44] V. Aulchenko,[1] T. Aushev,[11] T. Aziz,[36] A. M. Bakich,[35] V. Balagura,[11] M. Barbero,[6] I. Bedny,[1] U. Bitenc,[12] I. Bizjak,[12] A. Bondar,[1] M. Bračko,[7,18,12] J. Brodzicka,[25] T. E. Browder,[6] Y. Chao,[24] A. Chen,[22] B. G. Cheon,[2] R. Chistov,[11] S.-K. Choi,[5] Y. Choi,[34] Y. K. Choi,[34] A. Chuvikov,[30] S. Cole,[35] J. Dalseno,[19] M. Danilov,[11] M. Dash,[45] A. Drutskoy,[3] S. Eidelman,[1] D. Epifanov,[1] S. Fratina,[12] N. Gabyshev,[1] T. Gershon,[7] G. Gokhroo,[36] B. Golob,[17,12] H. C. Ha,[14] J. Haba,[7] Y. Hasegawa,[33] K. Hayasaka,[20] H. Hayashii,[21] M. Hazumi,[7] L. Hinz,[16] Y. Hoshi,[38] S. Hou,[22] W.-S. Hou,[24] Y. B. Hsiung,[24] T. Iijima,[20] A. Ishikawa,[7] M. Iwasaki,[40] Y. Iwasaki,[7] P. Kapusta,[25] T. Kawasaki,[27] H. R. Khan,[41] H. Kichimi,[7] H. J. Kim,[15] S. M. Kim,[34] K. Kinoshita,[3] S. Korpar,[18,12] P. Krokovny,[1] C. C. Kuo,[22] A. Kuzmin,[1] J. S. Lange,[4] G. Leder,[10] T. Lesiak,[25] A. Limosani,[7] S.-W. Lin,[24] D. Liventsev,[11] F. Mandl,[10] T. Matsumoto,[42] A. Matyja,[25] Y. Mikami,[39] W. Mitaroff,[10] K. Miyabayashi,[21] H. Miyata,[27] R. Mizuk,[11] Y. Nagasaka,[8] E. Nakano,[28] M. Nakao,[7] S. Nishida,[7] O. Nitoh,[43] S. Ogawa,[37] T. Ohshima,[20] S. Okuno,[13] S. L. Olsen,[6] H. Ozaki,[7] P. Pakhlov,[11] H. Palka,[25] C. W. Park,[34] H. Park,[15] K. S. Park,[34] L. S. Peak,[35] L. E. Piilonen,[45] A. Poluektov,[1] Y. Sakai,[7] N. Sato,[20] T. Schietinger,[16] O. Schneider,[16] A. J. Schwartz,[3] R. Seidl,[31] K. Senyo,[20] M. E. Sevior,[19] B. Shwartz,[1] V. Sidorov,[1] A. Somov,[3] R. Stamen,[7] M. Starič,[12] T. Sumiyoshi,[42] S. Y. Suzuki,[7] F. Takasaki,[7] N. Tamura,[27] M. Tanaka,[7] Y. Teramoto,[28] X. C. Tian,[29] K. Trabelsi,[6] T. Tsukamoto,[7] S. Uehara,[7] T. Uglov,[11] K. Ueno,[24] Y. Unno,[7] S. Uno,[7] P. Urquijo,[19] G. Varner,[6] K. E. Varvell,[35] S. Villa,[16] C. C. Wang,[24] C. H. Wang,[23] M.-Z. Wang,[24] E. Won,[14] Q. L. Xie,[9] B. D. Yabsley,[45] A. Yamaguchi,[39] Y. Yamashita,[26] M. Yamauchi,[7] J. Ying,[29] C. C. Zhang,[9] J. Zhang,[7] L. M. Zhang,[32] Z. P. Zhang,[32] and V. Zhilich[1]

(Belle Collaboration)

[1]*Budker Institute of Nuclear Physics, Novosibirsk*
[2]*Chonnam National University, Kwangju*
[3]*University of Cincinnati, Cincinnati, Ohio 45221*
[4]*University of Frankfurt, Frankfurt*
[5]*Gyeongsang National University, Chinju*
[6]*University of Hawaii, Honolulu, Hawaii 96822*
[7]*High Energy Accelerator Research Organization (KEK), Tsukuba*
[8]*Hiroshima Institute of Technology, Hiroshima*
[9]*Institute of High Energy Physics, Chinese Academy of Sciences, Beijing*
[10]*Institute of High Energy Physics, Vienna*
[11]*Institute for Theoretical and Experimental Physics, Moscow*
[12]*J. Stefan Institute, Ljubljana*
[13]*Kanagawa University, Yokohama*
[14]*Korea University, Seoul*
[15]*Kyungpook National University, Taegu*
[16]*Swiss Federal Institute of Technology of Lausanne, EPFL, Lausanne*
[17]*University of Ljubljana, Ljubljana*
[18]*University of Maribor, Maribor*
[19]*University of Melbourne, Victoria*
[20]*Nagoya University, Nagoya*
[21]*Nara Women's University, Nara*
[22]*National Central University, Chung-li*
[23]*National United University, Miao Li*
[24]*Department of Physics, National Taiwan University, Taipei*
[25]*H. Niewodniczanski Institute of Nuclear Physics, Krakow*
[26]*Nippon Dental University, Niigata*
[27]*Niigata University, Niigata*
[28]*Osaka City University, Osaka*
[29]*Peking University, Beijing*
[30]*Princeton University, Princeton, New Jersey 08544*
[31]*RIKEN BNL Research Center, Upton, New York 11973*
[32]*University of Science and Technology of China, Hefei*

[33]Shinshu University, Nagano
[34]Sungkyunkwan University, Suwon
[35]University of Sydney, Sydney NSW
[36]Tata Institute of Fundamental Research, Bombay
[37]Toho University, Funabashi
[38]Tohoku Gakuin University, Tagajo
[39]Tohoku University, Sendai
[40]Department of Physics, University of Tokyo, Tokyo
[41]Tokyo Institute of Technology, Tokyo
[42]Tokyo Metropolitan University, Tokyo
[43]Tokyo University of Agriculture and Technology, Tokyo
[44]University of Tsukuba, Tsukuba
[45]Virginia Polytechnic Institute and State University, Blacksburg, Virginia 24061
(Received 9 November 2005; published 20 February 2007)

We report the first observation of a charmoniumlike state recoiling from the J/ψ in the inclusive process $e^+e^- \to J/\psi$ + anything at a mass of $(3.943 \pm 0.006 \pm 0.006)$ GeV$/c^2$. We also observe the decay of this state into $D^*\bar{D}$ and determine its intrinsic width to be less than 52 MeV$/c^2$ at the 90% C.L. These results are obtained from a 357 fb^{-1} data sample collected with the Belle detector near the $\Upsilon(4S)$ resonance, at the KEKB asymmetric-energy e^+e^- collider.

DOI: 10.1103/PhysRevLett.98.082001 PACS numbers: 13.66.Bc, 12.38.Bx, 14.40.Gx

Recently, there have been a number of reports of new charmoniumlike states: $X(3872)$ [1], $Y(3940)$ [2], and $Y(4260)$ [3], that have not been assigned to any charmonium states in the conventional quark model [4]. Moreover, charmonium production in hadron interactions, $\gamma - \gamma$ fusion, and e^+e^- annihilation is not well described by theory. One striking example is the surprisingly large cross section for double charmonium production in e^+e^- annihilation [5,6]. These experimental results have generated renewed theoretical interest in the spectroscopy, decays, and production of charmonium.

In this Letter, we report the observation of a charmoniumlike state, which we denote as $X(3940)$, produced in the process $e^+e^- \to J/\psi X(3940)$, where other known charmonia are seen. $X(3940)$ decay to an open charm final state is also observed. The analysis is based on a 357 fb^{-1} sample collected by the Belle detector at the $\Upsilon(4S)$ resonance and nearby continuum at the KEKB asymmetric-energy e^+e^- collider.

The J/ψ reconstruction procedure is identical to our previously published analyses [5,7]. Oppositely charged tracks that are positively identified as muons or electrons are used for $J/\psi \to \ell^+\ell^-$ reconstruction. A partial correction for final state radiation and bremsstrahlung energy loss is performed by including the four-momentum of every photon detected within a 50 mrad cone around the electron direction in the e^+e^- invariant mass calculation. The two lepton candidate tracks are required to have a common vertex, with a distance from the interaction point in the plane perpendicular to the beam axis smaller than 1 mm ($\approx 6\sigma$). The $J/\psi \to \ell^+\ell^-$ signal region is defined by $|M(\ell^+\ell^-) - M_{J/\psi}| < 30$ MeV$/c^2$ ($\approx 2.5\sigma$) and the sideband by $[50, 250]$ MeV$/c^2$. J/ψ candidates in the signal window are subjected to a mass- and vertex-constrained fit to improve their momentum resolution. QED processes are substantially suppressed by requiring the total charged multiplicity ($N_{\rm ch}$) in the event to be greater than 4. Background due to J/ψ mesons from $B\bar{B}$ events is removed by requiring a center-of-mass (c.m.) momentum $p^*_{J/\psi} > 2.0$ GeV$/c$.

For the $X(3940) \to D^{(*)}\bar{D}$ study, we reconstruct D^0 candidates using decays to $K^-\pi^+$, K^-K^+, $K^-\pi^-\pi^+\pi^+$, $K^0_S\pi^+\pi^-$, and $K^-\pi^+\pi^0$, and D^+ candidates using $K^-\pi^+\pi^+$, $K^-K^+\pi^+$, and $K^0_S\pi^+$. A ± 15 MeV$/c^2$ mass window is used for all modes except $D^0 \to K^-\pi^-\pi^+\pi^+$ (± 10 MeV$/c^2$) and $D^0 \to K^-\pi^+\pi^0$ (± 20 MeV$/c^2$) ($\approx 2.5\sigma$ in each case). D candidates are refitted to the nominal D^0 or D^+ masses. To study the contribution of combinatorial background under the D peak, we use D sidebands with mass windows 4 times as large. For the $X(3940) \to J/\psi\omega$ search, candidate ω mesons are reconstructed from $\pi^+\pi^-\pi^0$ combinations within ± 20 MeV$/c^2$ ($\approx 2.5\sigma$) of the nominal ω mass.

We define the mass of the system recoiling against the reconstructed particle (F) as: $M_{\rm rec}(F) = \sqrt{(E_{\rm c.m.} - E^*_F)^2 - p^{*2}_F}$, where E^*_F and p^*_F are the c.m. energy and momentum of F, respectively. The $M_{\rm rec}(J/\psi)$ is shown in Fig. 1. Here, in addition to previously reported peaks at the η_c, χ_{c0}, and $\eta_c(2S)$ masses, there is a fourth enhancement around 3.94 GeV$/c^2$. The scaled J/ψ sideband distribution is shown by the hatched histogram. The open histogram represents the $\psi(2S) \to J/\psi X$ feed down, estimated from reconstructed $\psi(2S) \to J/\psi\pi^+\pi^-$ corrected for the $\psi(2S)$ reconstruction efficiency and $\mathcal{B}(\psi(2S) \to J/\psi X)/\mathcal{B}(\psi(2S) \to J/\psi\pi^+\pi^-)$. Both distributions exhibit no structure and, hence, can be described by smooth functions. Assuming that the fourth enhancement is due to a single resonance, we perform a binned likelihood fit to this spectrum that includes the three pre-

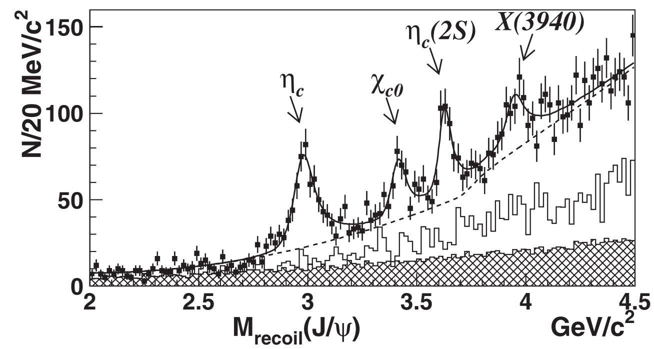

FIG. 1. The distribution of $M_{\rm rec}(J/\psi)$ in inclusive $e^+e^- \to J/\psi X$ events (points with error bars). The histograms and curves are described in the text.

viously seen charmonium states plus a fourth state. A typical signal $M_{\rm rec}(J/\psi)$ instrumental resolution is $\sim$30 MeV$/c^2$; the signal shape is further smeared by initial state radiation (ISR) resulting in a higher mass tail. The expected signal line shapes are determined from Monte Carlo (MC) simulation assuming no $\sqrt{s}$ dependence of the form factors (FF). The mass values for all states are free parameters in the fit, the widths of η_c and χ_{c0} are fixed to PDG values [8], and the $\eta_c(2S)$ width is fixed to 17 MeV$/c^2$ [9]. The $X(3940)$ width is a free parameter. The background is parametrized by a second order polynomial and a threshold term $[\sqrt{M_{\rm rec}(J/\psi) - 2M_D}]$ with a free normalization to allow for contributions from $e^+e^- \to J/\psi D\bar{D}$; thresholds for $J/\psi D^{(*)}\bar{D}^*$ are taken into account in the systematic uncertainties.

The fit results are given in Table I and shown in Fig. 1 as the solid curve; the dashed curve is the background function. We note that the masses of the known charmonium states are $\sim$10 MeV$/c^2$ lower than their nominal values. As the $M_{\rm rec}(J/\psi)$ scale has been calibrated using the process $e^+e^- \to \psi(2S)\gamma$ (the uncertainty due to J/ψ momentum reconstruction is $<$3 MeV$/c^2$ [7]), we ascribe these shifts to a combination of statistical fluctuations and systematic effects due to the high mass tails of the peaks. Varying the $\sqrt{s}$ dependence of the FF's in the MC simulation, we find shifts as large as 5 MeV$/c^2$. The systematic error in the η_c, χ_{c0}, and $\eta_c(2S)$ mass is thus estimated to be 6 MeV$/c^2$. The significance for each signal is defined as $\sqrt{-2\ln(\mathcal{L}_0/\mathcal{L}_{\rm max})}$, where $\mathcal{L}_0$ and $\mathcal{L}_{\rm max}$ denote the likelihoods returned by the fits with the signal

TABLE I. Summary of the signal yields, charmonium masses, and significances for $e^+e^- \to J/\psi(c\bar{c})_{\rm res}$.

$(c\bar{c})_{\rm res}$	N	M[GeV$/c^2$]	N_σ
η_c	501 ± 44	2.970 ± 0.005	15.3
χ_{c0}	230 ± 40	3.406 ± 0.007	6.3
$\eta_c(2S)$	311 ± 42	3.626 ± 0.005	8.1
$X(3940)$	266 ± 63	3.936 ± 0.014	5.0

yield fixed at zero and at the fitted value, respectively. The significance of the $X(3940)$ signal is 5.0σ. The fitted width of the $X(3940)$ state is consistent with zero within its large statistical error: $\Gamma = 39 \pm 26$ MeV$/c^2$.

The $X(3940)$ mass is above both the $D\bar{D}$ and the $D^*\bar{D}$ thresholds. We therefore perform a search for $X(3940)$ decays into $D\bar{D}$ and $D^*\bar{D}$ final states. Because of the small product of $D^{(*)}$ reconstruction efficiencies and branching fractions, it is not feasible to reconstruct fully the chain $e^+e^- \to J/\psi X(3940)$, $X(3940) \to D^{(*)}\bar{D}$. To increase the efficiency, we reconstruct the J/ψ and one D meson, detecting the other $\bar{D}^{(*)}$ as a peak in the $M_{\rm rec}(J/\psi D)$ spectrum. The MC simulation for $e^+e^- \to J/\psi D^{(*)}\bar{D}$ processes indicates a $M_{\rm rec}(J/\psi D)$ resolution of about 30 MeV$/c^2$ and a separation between these two processes of 2.5σ. Figure 2 shows the $M_{\rm rec}(J/\psi D)$ spectrum in the D mass window and the scaled D mass sidebands, where D includes D^0 and D^+. Some events have multiple D candidates. In these cases, only the candidate with invariant mass closest to the nominal D-meson mass is used. Two enhancements around the nominal D and D^* masses are clearly visible in this distribution. The excess of real D events compared to the D sidebands at masses above 2.1 GeV$/c^2$ is due to $e^+e^- \to J/\psi D^*\bar{D}^*$ or $J/\psi D^{(*)}\bar{D}^{(*)}\pi$ processes. A fit to this spectrum is performed using shapes fixed from MC simulation for three processes ($J/\psi D\bar{D}$, $J/\psi D^*\bar{D}$, and $J/\psi D^*\bar{D}^*$) and a second order polynomial. The fit gives $N_{D\bar{D}} = 86 \pm 17$ (5.1σ) and $N_{D^*\bar{D}} = 55 \pm 18$ (3.3σ) events in the D and the D^* peaks, respectively. Selecting events from the $M_{\rm rec}(J/\psi D)$ regions around the D and D^* masses ($\pm$70 MeV$/c^2$), we thus effectively tag the processes $e^+e^- \to J/\psi D\bar{D}$ and $J/\psi D^*\bar{D}$. The efficiencies of the D and D^* tag procedures are found from MC calculations to be independent of $M_{D\bar{D}^{(*)}}$ and equal to 0.097 in both cases, assuming equal fractions for $X(3940) \to D^{(*)0}\bar{D}^0$ and $D^{(*)+}D^-$.

We constrain $M_{\rm rec}(J/\psi D)$ to the $D^{(*)}$ nominal mass, improving the $M(D^{(*)}\bar{D}) \equiv M_{\rm rec}(J/\psi)$ resolution by a fac-

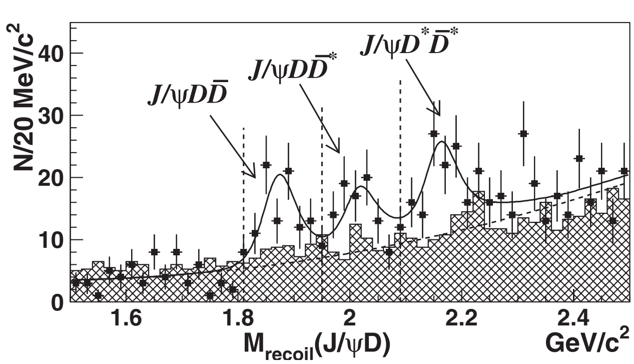

FIG. 2. The $M_{\rm rec}(J/\psi D)$ distribution for the D signal window (points with error bars). The hatched histogram corresponds to scaled D sidebands. The solid line shows the fit described in the text. The dashed line is the background function.

tor of 2.5 ($\sigma \sim 10$ MeV$/c^2$ after constraint), according to the MC simulation. In the $X(3940) \to D^*\bar{D}$ case, the reconstructed D either may be directly from the $X(3940)$ decay or may come from a $X(3940) \to D^* \to D$ cascade: the constraint $M_{\rm rec}(J/\psi D) \to M_{D^*}$ also works in the latter case, as both $X(3940) \to D^*\bar{D}$ and D^* decays have very little available phase space. The resulting $M_{\rm rec}(J/\psi)$ distributions are shown in Figs. 3(a) (M_D region) and 3(b) (M_{D^*} region). For events with multiple entries, the candidate with the invariant mass closest to the nominal D-meson mass is used. An $X(3940)$ peak with a resolution better than that for the unconstrained $M_{\rm rec}(J/\psi)$ distribution is evident in Fig. 3(b), corresponding to the decay $X(3940) \to D^*\bar{D}$. We perform a fit to this distribution. The signal function is a convolution of a Breit-Wigner function with a free width and a resolution function fixed to the MC expectation. The background function is a threshold function $[A + B \cdot M_{\rm rec}(J/\psi)]\sqrt{M_{\rm rec}(J/\psi) - M_{D^*} - M_D}$. The fit finds 24.5 ± 6.9 signal events with a statistical significance of 5.0σ. Separate fits to the $D^{*+}D^-$ and $D^{*0}\bar{D}^0$ distributions yield 7.2 ± 3.2 and 18.2 ± 6.0 signal events, respectively, in good agreement with the MC expectations (6.4 and 18.1) normalized to the integrated yield. The $X(3940)$ width is measured to be 15.4 ± 10.1 MeV$/c^2$, and its mass is 3.943 ± 0.006 GeV$/c^2$, in good agreement with the results of the inclusive fit. We perform a similar fit to the $M_{\rm rec}(J/\psi)$ distribution in Fig. 3(a). Since no signal is seen here, we fit this distribution with $X(3940)$ parameters fixed to the values found by the previous fit. The signal yield is found to be $0.2^{+4.4}_{-3.5}$ events, and we set an upper limit of 8.1 events at the 90% C.L.

An enhancement with a similar mass, $Y(3940)$, decaying into $J/\psi\omega$ has been recently observed by Belle [2] in B decays. We perform a search for the decay $X(3940) \to J/\psi\omega$ to see if $X(3940)$ and $Y(3940)$ could be the same particle. To increase the efficiency, we reconstruct the ω and only one J/ψ from the $J/\psi J/\psi\omega$ final state. The unreconstructed J/ψ is identified as a peak in the $M_{\rm rec}(J/\psi\omega)$ spectrum. A signal for $X(3940) \to J/\psi\omega$ would be seen as a peak near 3.94 GeV$/c^2$ in a distribution of $M_{\rm rec}(J/\psi) - M_{\rm rec}(J/\psi\omega) + M_{J/\psi}$ if the reconstructed J/ψ is prompt and in $M(J/\psi\omega)$ distribution if the reconstructed J/ψ is from the $X(3940)$ decay. Since the first case has a much larger combinatorial background and less sensitivity, we use only the second case. A scatterplot of $M_{\rm rec}(J/\psi\omega)$ vs $M(J/\psi\omega)$ in the data is shown in Fig. 4(a), and an $M(J/\psi\omega)$ projection with the additional requirement $|M_{\rm rec}(J/\psi\omega) - M_{J/\psi}| < 100$ MeV$/c^2$ in Fig. 4(b). A fit to this distribution is done with the signal parameters fixed from the result of the $D^*\bar{D}$ tagged fit; the background is a threshold function. The fit yields $1.9^{+3.2}_{-2.4}$ signal events corresponding to a 7.4 events upper limit at the 90% C.L.

The systematic errors for the $e^+e^- \to J/\psi X(3940)$ Born cross section and for the $X(3940)$ branching fractions are summarized in Table II. To estimate the systematic errors associated with the fitting procedure, we study the difference in $X(3940)$ yield returned by the fit to the $M_{\rm rec}(J/\psi)$ distribution under different assumptions for the signal and background parametrization. In particular, in the first fit we use a background function that includes several threshold functions corresponding to the production of $D^*\bar{D}$ and $D^*\bar{D}^*$ and the threshold function $[A + BM_{\rm rec}(J/\psi)]\sqrt{M_{\rm rec}(J/\psi) - M_{\rm thr}}$. We also include the $\chi_{c1(2)}$ states in the fit; upper limits on the contributions of these states were set in our previous study [7]. Different angular distributions result in different J/ψ (and D) reconstruction efficiencies. In the MC simulation, the J/ψ production angle and the J/ψ and $X(3940)$ helicity angle distributions are assumed to be flat. The extreme possible angular distributions are considered to estimate the systematic uncertainty of this assumption. This uncertainty par-

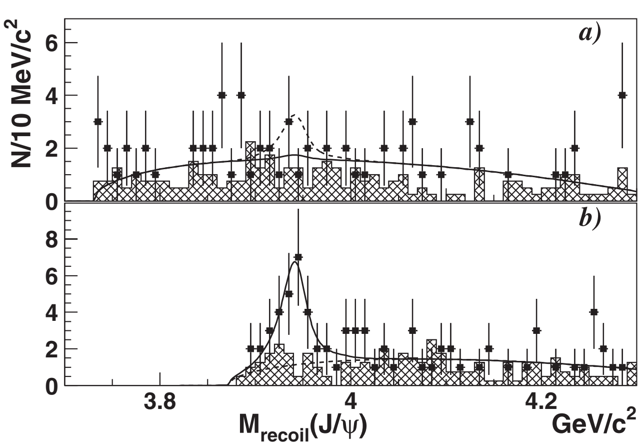

FIG. 3. The $M_{\rm rec}(J/\psi)$ distributions for events tagged and constrained as (a) $e^+e^- \to J/\psi D\bar{D}$ and (b) $e^+e^- \to J/\psi D^*\bar{D}$. The hatched histograms correspond to scaled D sidebands. The solid lines are result of the fits, described in the text. The dashed lines show (a) the 90% C.L. upper limit on the signal and (b) the background function.

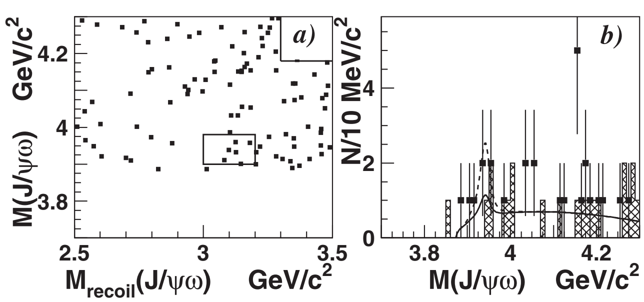

FIG. 4. (a) $M_{\rm rec}(J/\psi\omega)$ vs $M(J/\psi\omega)$, and (b) projection onto $M(J/\psi\omega)$, showing the contributions from the ω mass window (points with error bars) and sidebands [30 MeV$/c^2 <$ $|M(\pi^+\pi^-\pi^0) - M_\omega| < 50$ MeV$/c^2$, hatched histogram], the fit described in the text (solid line), and the 90% C.L. upper limit on the $X(3940) \to J/\psi\omega$ contribution (dashed line).

TABLE II. Contribution to the systematic error for $\sigma_{\rm Born}(e^+e^- \to J/\psi X(3940))$ and $\mathcal{B}(X(3940))$ [%].

Source	$\sigma_{\rm Born}$	$\mathcal{B}(X(3940))$		
		$D^*\bar{D}$	$D\bar{D}$	$J/\psi\omega$
Fitting procedure	±11	±17	⋯	⋯
Angular distributions	±19	±12	±12	±16
$N_{\rm ch}$ requirement	±3	±3	±3	±3
Reconstruction	±2	±6	±6	±5
Identification	±3	±1	±1	⋯
Total	±23	±22	±14	±17

tially cancels in the $\mathcal{B}(X(3940))$ due to the common J/ψ efficiency. Other contributions come from the $N_{\rm ch} > 4$ requirement, track reconstruction efficiency, and particle identification.

The $X(3940)$ mass and width are measured from the fit to the Fig. 3(b) distribution, as the resolution is much better there. The systematic errors of the $X(3940)$ mass are dominated by the 5 MeV/c^2 uncertainty associated with the fitting procedure, which is studied by varying the Breit-Wigner, signal resolution functions, and background parametrizations. The uncertainties due to FF's and momentum scale, even if one of these effects were responsible for mass shifts in the inclusive fit of the $M_{\rm rec}(J/\psi)$ distribution, are smaller due to the tagging and refit procedures. A conservative estimate of the FF's uncertainty is <2 MeV/c^2, obtained using MC simulation without an ISR contribution. The same MC simulation results in a 9 MeV/c^2 mass shift for the inclusive fit. The J/ψ momentum scale is verified in Ref. [7], but we conservatively estimate its systematic effect to be <3 MeV/c^2 by biasing the momentum scale to make a 10 MeV/c^2 mass shift for the inclusive fit. All of these contributions added in quadrature give a total uncertainty of 6 MeV/c^2. We estimate the $X(3940)$ width to be smaller than 47 MeV/c^2 at the 90% C.L.; this takes into account the fact that the likelihood function is not parabolic. When fitting systematics are taken into account, we find $\Gamma < 52$ MeV/c^2 at the 90% C.L.

The Born cross section for $e^+e^- \to J/\psi X(3940)$ is calculated following the procedure used in Ref. [7]. The Born cross section is 0.70 of the total cross section. Because of the $N_{\rm ch} > 4$ selection criterion, the analysis is not sensitive to $X(3940)$ decays producing two (or zero) charged tracks. We therefore present the result in terms of the product of the cross section and the branching fraction of the $X(3940)$ into more than two charged tracks ($\mathcal{B}_{>2}$):

$$\sigma_{\rm Born} \times \mathcal{B}_{>2} = (10.6 \pm 2.5 \pm 2.4)\ \text{fb}. \quad (1)$$

We calculate the fraction of $X(3940)$ decays with more than two charged tracks in the final state into $D^*\bar{D}$, $\mathcal{B}_{>2}(X(3940) \to D^*\bar{D})$. To remove the correlation between the inclusive and $D^*\bar{D}$ tagged samples, we apply a veto on $D^*\bar{D}$ tagging in the first sample. Taking into account the tagging efficiency, we find from the simultaneous fit to the $D^*\bar{D}$ tagged and vetoed inclusive spectra:

$$\mathcal{B}_{>2}(X(3940) \to D^*\bar{D}) = (96^{+45}_{-32} \pm 22)\% \quad (>45\% \quad \text{at 90\% C.L.}), \quad (2)$$

where the systematic errors are taken into account for the lower limit. In the limit of a vanishing fraction of low charged multiplicity $X(3940)$ decays, the measured value of $\mathcal{B}_{>2}$ corresponds to $\mathcal{B}(X(3940) \to D^*\bar{D})$. We set upper limits on the branching fractions of decay of $X(3940)$ into $D\bar{D}$ and $X(3940) \to J/\psi\omega$ final states, taking into account the estimated systematic errors:

$$\mathcal{B}(X(3940) \to D\bar{D}) < 41\% \quad \text{at 90\% C.L.}; \quad (3)$$

$$\mathcal{B}(X(3940) \to J/\psi\omega) < 26\% \quad \text{at 90\% C.L.} \quad (4)$$

These limits assume that low charged multiplicity $X(3940)$ decays are negligible and, thus, may be overestimated.

In summary, we have observed a charmoniumlike state at a mass of $(3.943 \pm 0.006 \pm 0.006)$ GeV/c^2, produced in the process $e^+e^- \to J/\psi X(3940)$, both in inclusive production and via the $X(3940) \to D^*\bar{D}$ decay mode. The combined significance of the signal using inclusive and D^*D tagged reconstruction, after vetoing the $D^*\bar{D}$ tagged events in the former sample, is found to be at least 5.9σ, taking into account the systematic errors. We have measured the Born cross section for the production process, the branching fraction for $X(3940) \to D^*\bar{D}$, and set upper limits on $X(3940)$ decays to $D\bar{D}$ and $J/\psi\omega$. The observed $X(3940)$ decay modes as well as its width indicate that it is probably not the same as $Y(3940)$, a state at approximately the same mass [2]. A possible interpretation of $X(3940)$ as $\eta_c(3S)$ is discussed in Ref. [4]. $\chi_{c0}(2P)$ cannot decay to $D^*\bar{D}$ and therefore does not contribute to the $D^*\bar{D}$ tagged peak. However, a contribution to the inclusive $M_{\rm rec}(J/\psi)$ distribution is not excluded. Our results on the η_c, χ_{c0}, and $\eta_c(2S)$ mass supersede those of Refs. [5,7].

We thank the KEKB group for the excellent operation of the accelerator, the KEK cryogenics group for the efficient operation of the solenoid, and the KEK computer group and the NII for valuable computing and Super-SINET network support. We acknowledge support from MEXT and JSPS (Japan); ARC and DEST (Australia); NSFC (Contract No. 10175071, China); DST (India); the BK21 program of MOEHRD and the CHEP SRC program of KOSEF (Korea); KBN (Contract No. 2P03B 01324, Poland); MIST (Russia); MHEST (Slovenia); SNSF (Switzerland); NSC and MOE (Taiwan); and DOE (U.S.A.).

[1] S. K. Choi *et al.* (Belle Collaboration), Phys. Rev. Lett. **91**, 262001 (2003); D. Acosta *et al.* (CDF Collaboration),

Phys. Rev. Lett. **93**, 072001 (2004); V. M. Abazov *et al.* (D0 Collaboration), Phys. Rev. Lett. **93**, 162002 (2004); B. Aubert *et al.* (*BABAR* Collaboration), Phys. Rev. D **71**, 071103 (2005).
[2] S. K. Choi *et al.* (Belle Collaboration), Phys. Rev. Lett. **94**, 182002 (2005).
[3] B. Aubert *et al.* (*BABAR* Collaboration), Phys. Rev. Lett. **95**, 142001 (2005).
[4] E. J. Eichten, K. Lane, and C. Quigg, Phys. Rev. D **73**, 014014 (2006); **73**, 079903(E) (2006).
[5] K. Abe *et al.* (Belle Collaboration), Phys. Rev. Lett. **89**, 142001 (2002).
[6] B. Aubert *et al.* (*BABAR* Collaboration), Phys. Rev. D **72**, 031101 (2005).
[7] K. Abe *et al.* (Belle Collaboration), Phys. Rev. D **70**, 071102 (2004).
[8] S. Eidelman *et al.* (Particle Data Group), Phys. Lett. B **592**, 1 (2004).
[9] B. Aubert *et al.* (*BABAR* Collaboration), Phys. Rev. Lett. **92**, 142002 (2004).